Comparison of Vector and Matrix Format Tangential Interpolation for FDNE

Gurunath Gurrala[1,*], Kiran Kumar Challa[1]

Department of Electrical Engineering, Indian Institute of Science, Bengaluru, India

Abstract

Vector format tangential interpolation (VFTI) framework for deriving controllable and observable descriptor state space model using Loewner matrix pencil from the transfer matrix data has been recently proposed for VLSI circuits. It uses data sampled directionally i.e. two columns or two rows of the transfer matrix, called tangential interpolation data. In VFTI the information contained in the frequency samples is not fully utilized and the accuracy gets affected with large number of samples. Matrix format tangential interpolation (MFTI) has been proposed as an enhancement to VFTI in the literature which uses the entire transfer matrix so that all the information contained in the samples is fully utilized. This paper investigates the applicability of MFTI for state space modeling of power system FDNEs and proposes a novel MATLAB® based implementation for Loewner matrix construction. Properties of MFTI such as convergence speed, accuracy, stability and passivity are compared with vector fitting (VF) and VFTI. Impact of number of samples is also studied.

Keywords: Tangential interpolation, Loewner Matrix, Vector fitting, Frequency Dependent Network Equivalents, EMTP

1. Introduction

Network equivalents are very useful tools for analyzing network transients, lightning impacts, network interactions with the advanced control systems etc. in large power networks [1]. The frequency dependent admittance or impedance of a network that needs to be simplified in electromagnetic transient studies is usually modeled as a frequency dependent network equivalent (FDNE). These are usually modeled either as a lumped parameter circuit model or as a rational function model [1]. Various types of equivalents are needed for studying different types of phenomenon. A good survey of these equivalents and their modeling techniques are reported in [1]. In [2], early methods of FDNEs have been summarized.

Rational function approximation of FDNEs using vector fitting has seen significant growth [3] in the last decade. Ill-conditioning issues in FDNEs are addressed using frequency partitioning in [4, 5, 6]. A multi-port FDNE based on time domain simulations is proposed in [7]. Several variations of vector fitting are discussed for FDNE's in [8, 3, 9]. Vector fitting needs good initialization for successful pole-relocation and needs separate passivity enforcement in some conditions. In [10], a new method for initialization of poles is proposed. In [11], a matrix pencil based method is proposed for rational function approximation of frequency responses.

Loewner matrix pencil based tangential interpolation framework is proposed in [12] to construct a controllable and observable state space model from the transfer matrix data. Data of the transfer matrix sampled directionally called tangential interpolation data is used in these models. Recently, a multi-port modelling technique is proposed in [13, 14] for VLSI systems with higher number of terminals. This method uses two vectors which sample only two columns or rows of the transfer matrix, hence referred as vector format tangential interpolation (VFTI) [15]. VFTI is originally proposed with a half samples data splitting scheme for tangential data. In [16], VFTI is investigated for the modeling of power system FDNEs and shown that alternate samples data splitting is more accurate than half samples data splitting. In [17], it has been shown that VFTI loses accuracy with large number of samples. However, this is concluded using the half samples data splitting and no attempt is made to optimize the Loewner matrix construction. A matrix format tangential interpolation (MFTI) is proposed in [17] as an enhancement to VFTI with half samples data splitting. MFTI uses the entire transfer matrix sample instead of two sampled vectors there by all the information contained in the transfer matrix is fully utilized for better accuracy. MFTI requires only $1/p$ samples to recover the system compared to VFTI where p is the number of ports. MFTI is non-iterative, robust, results in stable fitted models and do not require pole initialization like vector fitting. The order of the system can be approximately recognized from the

singular values of Loewner matrix pencil.

Because of the above compelling advantages, applicability of the MFTI for the modeling of power system FDNEs is explored in this paper by comparing its performance with vector fitting (VF) and VFTI. In this paper, a novel MATLAB® based implementation for Loewner matrix construction is proposed to improve the convergence speed of MFTI. The MFTI is compared with VFTI using alternate samples data splitting and also with widely used vector fitting. Two representative power system examples have been used for performance comparison.

2. Matrix format tangential interpolation

The goal of tangential interpolation [12] is to construct an observable and controllable generalized linear time invariant (LTI) descriptor system with m-inputs, p-outputs and n-internal variables of the form Σ from frequency response of $H(s)$ for a frequency range of $\{s_{min}, s_{max}\}$.

$$\Sigma : \begin{cases} E\dot{x}(t) = Ax(t) + Bu(t) \\ y(t) = Cx(t) + Du(t) + Y^\infty \dot{u}(t) \end{cases} \quad (1)$$

where $x(t)$ is a state vector (if E is singular and invertible), $u(t)$ is input, $y(t)$ is output. While E, $A\epsilon R^{n \times n}$, $B\epsilon R^{n \times m}$, $C\epsilon R^{p \times n}$, D, $Y^\infty \epsilon R^{n \times n}$ are constants. Transfer function $H(s)$ of Σ is expressed as

$$H(s) = \underbrace{C(sE - A)^{-1}B}_{Regular\ Part} + \underbrace{D + sY^\infty}_{Irregular\ Part} \quad (2)$$

Sample data of $H(s)$ is $\{H(s_1), ..., H(s_P)\}$ at set points $S = \{s_1, ..., s_P\}$ which are partitioned as

$$S = \{\lambda_1, ..., \lambda_k\} \cup \{\mu_1, ..., \mu_h\}. \quad (3)$$

The sampled data can be of scalar data, matrix data or tangential data (matrix data sampled directionally on the left and on the right) [12]. Using the k samples of $H(s)$ (Y/Z matrix in this application) at k frequency points, the matrix format right tangential data is constructed as [17]

$$\{\lambda_i, R_i, W_i | \lambda_i = j2\pi f_i, W_i = H(f_i) R_i \ for \ i = 1, 3..k - 1;$$
$$\lambda_i = -\lambda_{i-1}, R_i = R_{i-1}, W_i = \bar{W}_{i-1} \ for \ i = 2, 4....k\} \quad (4)$$

The matrix format left tangential data is constructed as

$$\{\mu_i, L_i, V_i | \mu_i = j2\pi f_{i+1}, V_i = L_i H(f_{i+1}) \ for \ i = 1, 3..k - 1;$$
$$\mu_i = -\mu_{i-1}, L_i = L_{i-1}, V_i = \bar{V}_{i-1} \ for \ i = 2, 4....k\} \quad (5)$$

where $\lambda_i, \mu_i \epsilon \{\pm 2\pi f_i\}$. Matrices W_i and V_i are right and left interpolation data. R_i and L_j are called right and left tangential directions. Tangential data can be represented in a more compact matrix form as

$$\Lambda = diag[\underbrace{\lambda_1, .., \lambda_1}_{t_1}, \underbrace{-\lambda_1, .., -\lambda_1}_{t_2}, ..., \underbrace{\lambda_{k-1}, .., \lambda_{k-1}}_{t_{k-1}}, \underbrace{-\lambda_{k-1}, ..., -\lambda_{k-1}}_{t_k}]$$

$$R = [R_1^{m \times t_1}, R_1^{m \times t_2}, ..., R_{k-1}^{m \times t_{k-1}}, R_{k-1}^{m \times t_k}]$$

$$W = [W_1^{p \times t_1}, \overline{W}_1^{p \times t_2}, ..., W_{k-1}^{p \times t_{k-1}}, \overline{W}_{k-1}^{p \times t_k}]$$

$$M = diag[\underbrace{\mu_1, ..., \mu_1}_{t_1}, \underbrace{-\mu_1, .., -\mu_1}_{t_2}, ..., \underbrace{\mu_{k-1}, .., \mu_{k-1}}_{t_{k-1}}, \underbrace{-\mu_{k-1}, .., -\mu_{k-1}}_{t_k}]$$

$$(6)$$

$$L = \begin{bmatrix} L_1^{t_1 \times p} \\ L_1^{t_2 \times p} \\ \vdots \\ L_{k-1}^{t_{k-1} \times p} \\ L_{k-1}^{t_k \times p} \end{bmatrix}, V = \begin{bmatrix} V_1^{t_1 \times m} \\ \overline{V}_1^{t_2 \times m} \\ \vdots \\ V_{k-1}^{t_{k-1} \times m} \\ \overline{V}_{k-1}^{t_k \times m} \end{bmatrix}, \quad (7)$$

where $t_1 = t_2, t_3 = t_4, ..., t_{k-1} = t_k$. For systems with $m = p$, if $t_i = m$ and $rank(L_i) = rank(R_i) = t_i (for \ i = 1, 2, ...k)$, then all entries in the transfer matrices are used for interpolation. t_i can be adjusted to decide between speed and accuracy and/or to assign different weights to ill-conditioned samples [17]. In MFTI these are usually selected as $p \times p$ identity matrices for a p-port network. The transfer function (2) obtained using interpolation method satisfies the following right and left conditions by finding a minimal realization $[E, A, B, C, D]$ for tangential data

$$H(\lambda_i) R_i = W_i$$
$$L_j H(\mu_j) = V_j \quad (8)$$

The choice of identity matrices as interpolation vectors simplifies the above constraints as

$$H(\lambda_i) = W_i$$
$$H(\mu_j) = V_j \quad (9)$$

Thus the entire H(s) matrix is used at every frequency point [15, 17]. The tangential interpolation framework uses *Loewner matrix* ($\mathcal{L}$) and the *shifted Loewner matrix* ($\sigma \mathcal{L}$) as the underlying tools for the solution because these matrices have a system theoretically significant factorization [12, 17]. Using the directions R_i and L_j, Loewner matrix ($\mathcal{L}$) of $H(s)$ can be built as follows

$$\mathcal{L} = \begin{bmatrix} \frac{V_1 R_1 - L_1 W_1}{\mu_1 - \lambda_1} & \cdots & \frac{V_1 R_k - L_1 W_k}{\mu_1 - \lambda_k} \\ \vdots & \ddots & \vdots \\ \frac{V_h R_1 - L_h W_1}{\mu_h - \lambda_1} & \cdots & \frac{V_h R_k - L_h W_k}{\mu_h - \lambda_k} \end{bmatrix} \quad (10)$$

Similarly shifted Loewner matrix ($\sigma \mathcal{L}$) of $sH(s)$ can be built as follows

$$\sigma \mathcal{L} = \begin{bmatrix} \frac{\mu_1 V_1 R_1 - \lambda_1 L_1 W_1}{\mu_1 - \lambda_1} & \cdots & \frac{\mu_1 V_1 R_k - \lambda_k L_1 W_k}{\mu_1 - \lambda_k} \\ \vdots & \ddots & \vdots \\ \frac{\mu_h V_h R_1 - \lambda_1 L_h W_1}{\mu_h - \lambda_1} & \cdots & \frac{\mu_h V_h R_k - \lambda_k L_h W_k}{\mu_h - \lambda_k} \end{bmatrix} \quad (11)$$

In MFTI, the elements $[\mathcal{L}_{i,j}], [\sigma \mathcal{L}_{i,j}]$ are block matrices of size $p \times p$ and the size of $\mathcal{L}, \sigma \mathcal{L}$ is $np \times np$.

Similar to VFTI, MFTI data satisfies the following Sylvester equations.

$$\mathcal{L}\Lambda - M\mathcal{L} = LW - VR \quad (12)$$
$$\sigma \mathcal{L}\Lambda - M\sigma \mathcal{L} = LW\Lambda - MVR \quad (13)$$

The Loewner matrix is factored as a product of the generalized controllability and generalized observability matrices. The derivation can be found in [12, 13]. The pair

(E, A, B) is controllable and (C, E, A) is observable, so by appropriately choosing the sampling directions R_i and L_j, the rank of the Loewner matrix is same as the rank of E matrix, while the rank of the shifted Loewner matrix is $+p$ more than the rank of A matrix [12, 13]. The state space realization can be obtained from the singular value decomposition (SVD) of $\mathcal{L}$ [12, 13] as shown below

$$
\begin{aligned}
E &= -Y_1^* L X_1, \\
A &= -Y_1^* \Sigma L X_1 \\
B &= Y_1^* V; \\
C &= W X_1; \\
D &= 0;
\end{aligned}
\tag{14}
$$

where

$$
\begin{aligned}
&\forall x \in S \\
&SVD(x\mathcal{L} - \sigma\mathcal{L}) = Y_1 \Sigma X_1^*;
\end{aligned}
\tag{15}
$$

The pencil $(\sigma\mathcal{L}, \mathcal{L})$ loses rank only when x is one of its eigenvalues [13], so choice of x would not be an issue. One can identify the order of the underlying system based on a large drop in the singular values of $(x\mathcal{L} - \sigma\mathcal{L})$.

3. MFTI implementation

This section describes the implementation details of the MFTI using MATLAB® syntax.

Step 1: *Reading frequency response data*
A p-port system admittance/impedance matrix $H(s)$ sampled at frequencies $S = \{s_1, s_2..., s_{N_s}\}$, can be represented in MATLAB® as a $p \times p \times N_s$ matrix, where $s_i = j\omega_i$. Even number of samples are assumed without loss of generality. MFTI only needs $1 : p : N_s$ samples. So only $N = N_s/p$ samples will be used. The required data is obtained as
$$
\begin{aligned}
H_1 &= H(:,:,1:p:N_s) \\
S_1 &= S(1:p:N_s)
\end{aligned}
$$

Step 2: *Generation of even and odd samples*
The required data H_1, S_1 need to be separated into even and odd samples as follows
$$
\begin{aligned}
S_\lambda &= S_1(1:2:end,1) \\
S_\mu &= S_1(2:2:end,1) \\
H_\lambda(s) &= H_1(S_\lambda) \\
H_\mu(s) &= H_1(S_\mu)
\end{aligned}
$$

Step 3: *Calculation of W and V matrices*
A real system should satisfy $H(s) = H(\bar{s})$. Therefore in (4), W_i, V_i are built in such a way that the Y-parameters at the complex conjugate values of the sample points $-j\omega_i$ are equal to the complex conjugates of the measurements at $j\omega_i$. This is done in MATLAB® as follows

$$
\begin{aligned}
\mu(1:2:N,1) &= S_\mu \\
\mu(2:2:N,1) &= -S_\mu \\
\lambda(1:2:N,1) &= S_\lambda \\
\lambda(2:2:N,1) &= -S_\lambda
\end{aligned}
$$
$$
\begin{aligned}
&\textbf{for } \mathbf{kk = 1:N/2} \\
&\quad V1 = squeeze(H_\mu(:,:,kk)) \\
&\quad V = [V; V1; conj(V1)] \\
&\quad W1 = squeeze(H_\lambda(:,:,kk)) \\
&\quad W = [W, W1, conj(W1)] \\
&\textbf{end}
\end{aligned}
$$

Step 4: *Construction of tangential data*
After the V, W matrices are constructed, the tangential data need to be constructed as in (4) to solve Sylvester equations for forming Loewner ($\mathcal{L}$) and shifted Loewner ($\sigma\mathcal{L}$) matrices. Alternately, $\mathcal{L}$ and $\sigma\mathcal{L}$ can be formed using $for-loops$ from individual components of tangential data matrices. It is found that both the approaches become computationally expensive when the number of samples increase. In MFTI, since R_i, L_i are identity matrices, the numerator of ($\mathcal{L}$) is $(V_j - W_i)/\mu_j - \lambda_i$ where j changes in rows from $j = 1$ to $j = k$ and i changes in columns from $i = 1$ to $i = k$. So this can be obtained by stacking V, μ matrices horizontally and W, λ matrices vertically. This can be done efficiently using MATLAB® *repmat* command. One has to remember that each element of μ, λ will be multiplying $p \times p$ matrix elements of W, V. So we first define μ_1, λ_1 which are matrices formed by the replacement of singleton elements of μ, λ with respective $p \times p$ matrix elements. Then we define μ_2, λ_2 which are respective stacked matrices as shown below

$$
\begin{aligned}
&\mu_1 = [\ ] \\
&\lambda_1 = [\ ] \\
&\textbf{for } \mathbf{kk = 1:N} \\
&\quad \mu_1 = [\mu_1; ones(noports, noports) * \mu(kk)] \\
&\quad \lambda_1 = [\lambda_1, ones(noports, noports) * \lambda(kk)] \\
&\textbf{end} \\
&\mu_2 = repmat(\mu_1, 1, N) \\
&\lambda_2 = repmat(\lambda_1, N, 1) \\
&V_{stack} = repmat(V, 1, N) \\
&W_{stack} = repmat(W, N, 1)
\end{aligned}
$$

Step 5: *Construction of $\mathcal{L}$ and $\sigma\mathcal{L}$*
The loewner and shifted loewner matrices can be constructed efficiently without using $for-loops$ or solution of Sylvester equations as shown below

$$
\begin{aligned}
\mathcal{L} &= (V_{stack} - W_{stack})./(\mu_2 - \lambda_2) \\
\sigma\mathcal{L} &= (\mu_2.*V_{stack} - \lambda_2.*W_{stack})./(\mu_2 - \lambda_2)
\end{aligned}
$$

3

This is a novel implementation for Loewner and shifted Loewner matrix construction to improve the convergence speed of MFTI in this paper.

Step 6: The remaining steps after construction of $\mathcal{L}$ & $\sigma\mathcal{L}$ are same as VFTI and they are repeated in APPENDIX for the sake of completeness.

The following error measures [13] are used for quantifying the performance of MFTI,

$$\mathcal{H}_\infty \, error = \frac{\max_{i=1...,N_s} \sigma_1 \left(Y^{(i)} - H_{fit} \left(j2\pi f_i \right) \right)}{\max_{i=1...,N_s} \sigma_1 \left(Y^{(i)} \right)} \quad (16)$$

$$\mathcal{H}_2 \, error = \sqrt{\frac{\sum_{i=1}^{N_s} \left\| Y^{(i)} - H_{fit} \left(j2\pi f_i \right) \right\|_F^2}{\sum_{i=1}^{N_s} \left\| Y^{(i)} \right\|_F^2}} \quad (17)$$

The first error measure is the normalized $\mathcal{H}_\infty - norm$ which evaluates the maximum deviation in the singular values. and second one is the normalized $\mathcal{H}_2 - norm$ which evaluates the error in all entries, a good estimate of the overall performance.

4. Comparison of VFTI, MFTI and vector fitting

In this section, state space models for frequency response data of two representative power system examples is derived using MFTI and its performance is compared with the vector fitting and VFTI. Alternate samples data splitting is used for VFTI because it is more accurate than the half samples data splitting which was originally proposed for VFTI [16]. This study uses matrix fitting toolbox1 from the vector fitting web site [18, 19, 20]. Passivity over the entire frequency range is tested using $eig(Re\{Y(s)\}) > 0$ [21]. Passivity is also checked using time domain simulations, for a unit step voltage excitation at port-1 through a 5Ω resistor with other ports open using the discretization scheme proposed in [22].

4.1. Test System 1: FDNE of an electrical distribution system

Consider a power distribution system shown in Fig.1 with two 3-phase terminals (A, B) [3]. The 6×6 admittance matrix $Y(s)$ with respect to A & B terminals is fitted with MFTI, VFTI and VF approaches. The data is taken from [18]. This data set has 300 frequency samples in the frequency range 10 Hz - 100 kHz. Fig.2a shows the singular values of $x\mathcal{L} - \sigma\mathcal{L}$ from which the approximate order of the system can be identified. The singular values of both the VFTI and MFTI approaches are close to each other. The largest singular value drop is not very evident in the plots. However, a gradual change in the slope is clearly visible in the circled area. This is because of the infinite
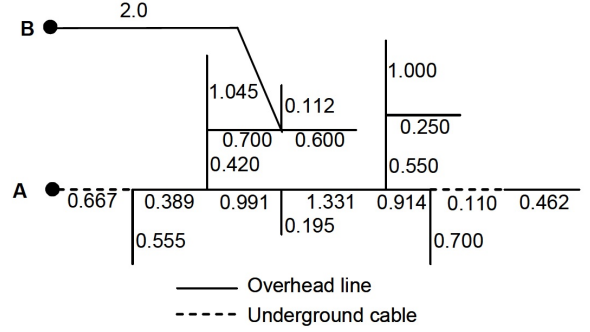

Figure 1: Test System 1, Power Distribution Network

dimensional distributed parameter model of the distribution line [15]. The order of the system for vector fitting is taken as 60. From the singular value plots orders 70 and 76 are selected respectively for VFTI and MFTI corresponding to the largest drop in the circled region. The actual orders of the system are 55, 61 for VFTI, MFTI respectively after extracting the irregular part.

The results of the fitting for all elements are shown in Fig.2b along with the error in all the fitting methods with respect to original data in Fig.2c. It can be observed that fitting responses with VFTI and MFTI are accurate and comparable to vector fitting. Magnitude of error in case of VFTI and MFTI is in the order of 10^{-4} or less for all the frequencies. They are indistinguishable because they overlap with each other.

The eigenvalues of $Re\{Y\}$ over the wide frequency range are shown in Fig.3a. No passivity violations are found. The time domain responses, current through phase-a of port-A and Voltage at phase-a of port-B, for a unit step voltage applied at the phase-a of port-A with other port-B open is shown in Fig.3b and Fig.3c respectively. Stable time domain simulations are obtained. All the FDNEs are implemented as state space models as in [22]. So all the time domain simulations took more or less similar execution times.

Table 1: Comparison of VFTI, MFTI & VF: Test System 1

Method	H_2 error	H_∞ error	Order	Passive	Fitting Time, s
VFTI	0.0037	0.0085	55	Yes	0.28
MFTI	0.0035	0.0033	61	Yes	0.23
VF	0.0003	0.0003	60	Yes	0.8834

The performances of all the three methods are shown in Table 1. The error measures of MFTI, VFTI are comparable to vector fitting. The system orders after irregular part extraction are also shown in the table. The execution times of the programs in fitting the FDNEs are also shown in the table. The results are based on a laptop equipped with Intel core i7-3632QM quad core 2.2GHz processor with 8GB RAM. It can be observed that MFTI is faster than VFTI and vector fitting.
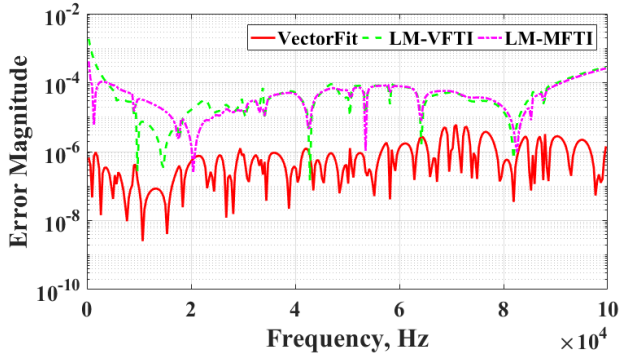
Fig.4 shows the frequency response of the system with full samples and 1/p samples. It can be observed that several peaks and valleys are missing in the 1/p samples plot. However, the MFTI has fitted the responses very accurately. This shows the superior interpolation capabilities
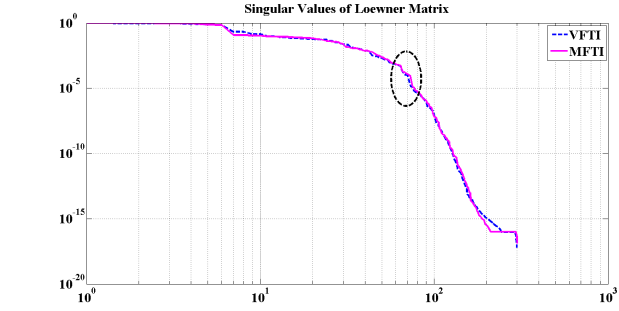
(a) Singular Values
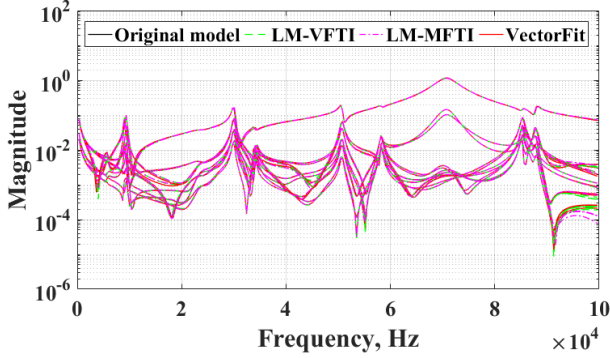
(b) Frequency Response

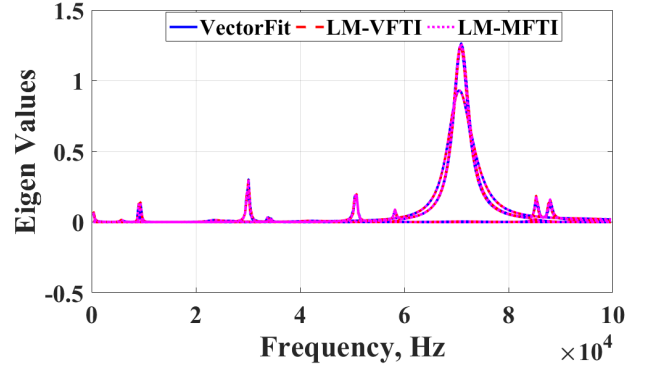
(c) Errors in the Fitted Frequency Response

Figure 2: Singular values of $x\mathcal{L} - \sigma\mathcal{L}$ and Frequency response of Y(s): Test System 1

(a) Eigenvalues of $Re(Y)$
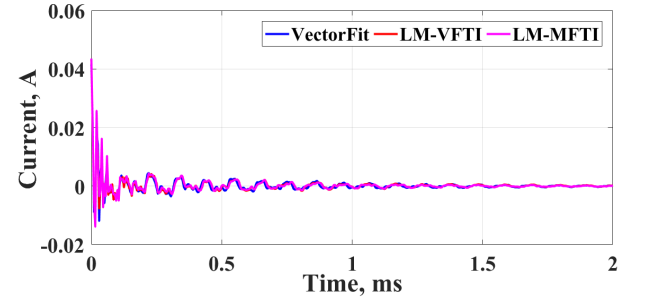

(b) Current through Phase-a of Port-A

(c) Voltage at Phase-a of Port-B

Figure 3: Eigenvalues of $Re\{Y\}$ and Time domain results: Test System 1

Figure 4: $Y(s)$ with all samples and 1/p samples: Test System 1

of the MFTI method.

4.2. Test System 2: 500kV Transmission Network

FDNE for studying the switching transient on TL4 while closing CB1 of the 500kV test system shown in Fig.5 is obtained by MFTI in this subsection. The lower part seen from Bus A is represented in detail as study zone of the system. The remaining upper part need to be replaced by an FDNE. The system data is available in [4]. The admittance matrix of the external network is calculated between 0 Hz and 10 kHz with 2000 equidistant frequency points [4]. The data is obtained from the author of [4].
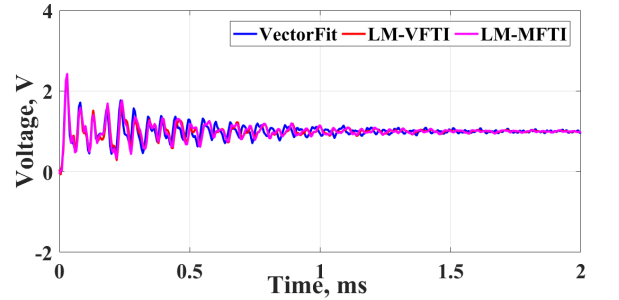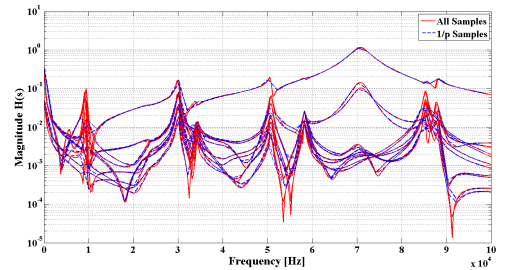
The singular values of the Loewner matrix shown in Fig.6a doesn't show large sudden drop. Only a gradual change in the slope of the singular values observed and shown in the circled area which starts around 100 Hz. Orders 155,164 are selected for MFTI and VFTI whereas the vector fitting produces an accurate passive fit with order 150.

The frequency response fits of elements Y(1,1) and Y(1,2) for all methods are shown in Fig.6b along with the error in all the fitting methods with respect to original data in Fig.6c. Both VFTI and MFTI methods fitted ac-
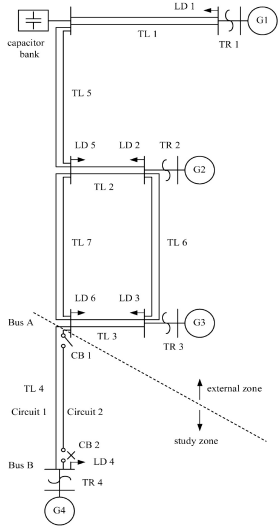
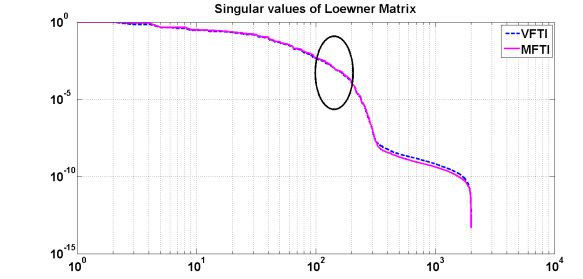Figure 5: Test System 2, 500kV Transmission Network

(a) Singular Values

(b) Frequency Response

(c) Errors in the Fitted Frequency Responses

Figure 6: Singular values of $x\mathcal{L} - \sigma\mathcal{L}$ and Frequency response of Y(1,1), Y(1,2): Test System 2

curate models comparable to vector fitting. As the plots are over lapping it is difficult to distinguish them. Errors in case of VFTI and MFTI for this case are similar to that of the VF. The passivity of the fitted models can be verified from the eigenvalues of $Re\{Y\}$ and the time domain simulations shown in Fig.7b and Fig.7c respectively. It can be observed that there are no passivity violations and the simulations are stable.

Table 2 summarizes the performances of the three methods for test system 2. Here also the MFTI is found to be faster than VFTI but slower than vector fitting because of the large number of samples. The order of MFTI is slightly higher and accuracy measures are comparable.

Table 2: Comparison of VFTI, MFTI & VF:Test System 2

| Method	H_2 error	H_∞ error	Order	Passive	Fitting Time, s
VFTI	0.0302	0.081	150	Yes	17.69
MFTI	0.028	0.069	156	Yes	16.45
VF	0.0004	0.0039	150	Yes	5.9

In [15, 17], MFTI was shown to be superior to VFTI with half samples data splitting. Since this paper used the alternate samples data splitting proposed in [16], the accuracy measures of MFTI and VFTI are turned out to be closer in the two examples. MFTI is found to be faster than VFTI and vector fitting with comparable accuracy for sample sizes of 300 or lower. When the number of samples are increased beyond that MFTI apparently produced slightly higher order models faster than VFTI, but slower than vector fitting. The VFTI in this paper is implemented using an efficient Loewner matrix formation proposed in [16]. So the speedup of MFTI is not very significant as claimed in [17] with large number of samples. This is because the singular value decomposition becomes expensive with increase in sample size. In all these cases MFTI and VFTI have shown similar singular value drops. The order of the system has been identified from a region corresponding to the gradual change in slope of the singular values.
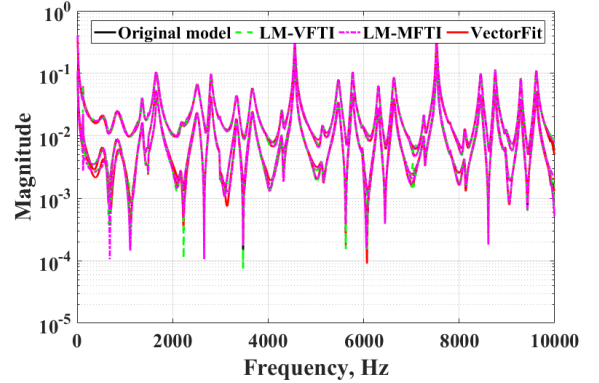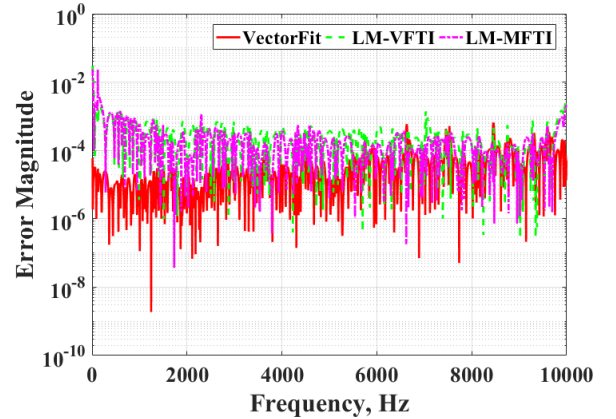
In vector fitting, the order determination takes considerably large number of trials compared to MFTI. It is advantageous to use MFTI over VFTI because of the less number of samples and better accuracy. The advantage of less number of samples will be more pronounced with large number of ports [17]. No passivity violations are observed in the test systems used. However, Loewner frameworks do not guarantee passivity and for any violations, passivity enforcement can be done using the methods proposed in [23]. The difference in errors of the fitted frequency responses will emerge as small deviations in time domain simulations. Investigations on the application of proposed technique to higher frequencies above 100 kHz also can be carried out. It is envisioned that further research in
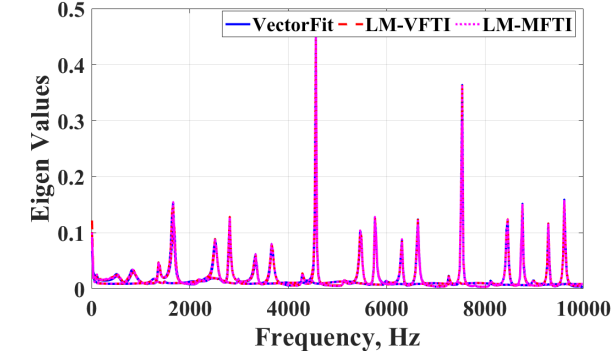
(a) Eigenvalues $Re(Y)$
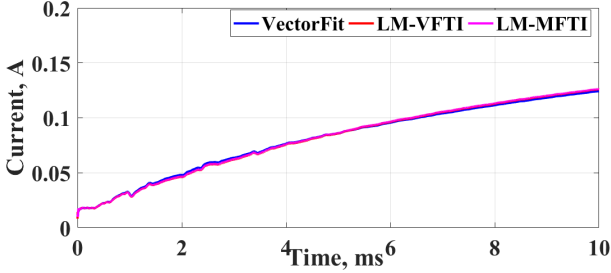
(b) Current through port1
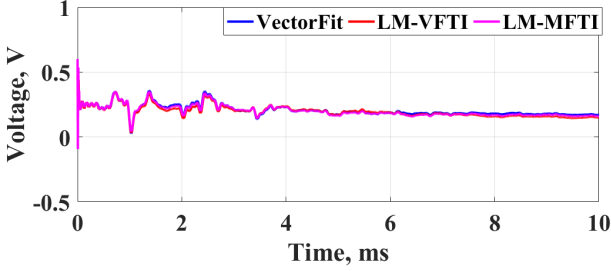
(c) Voltage at port 2

Figure 7: Eigenvalues of $Re\{Y\}$ and Time domain results: Test System 2

these directions will make the Loewner matrix approaches, MFTI and VFTI, a viable alternatives to iterative methods.

5. Conclusions

The frequency dependent network equivalents are indispensable in electromagnetic transient simulations of large power systems. This paper presents the application of matrix format tangential interpolation method for FDNE modeling of power systems and compares it's performance with VF and VFTI. A novel MATLAB® based implementation for Loewner matrix construction is proposed to improve the convergence speed of MFTI. Following are the key observations from the comparison,

- The impact of number of data samples is studied and MFTI uses less number of samples than VF and VFTI.

- MFTI has shown superior interpolation properties

in-spite of loss of several peaks and valleys due to $1/p$ samples.

- It is found that MFTI is faster than VFTI irrespective of sample size. MFTI is shown to be faster than vector fitting for sample sizes 300 or lower. Further research is needed to improve the speed of MFTI with large number of samples.

- MFTI approach is shown to be accurate and stable for all the test systems studied.

Appendix A.

The MATLAB® implementation steps after the construction of Loewner and shifted Loewner matrices are same as VFTI. They are repeated here from [16] for completeness.

Step 6a: *Obtain real $\mathcal{L}$ & $\sigma\mathcal{L}$*
The following steps convert $\mathcal{L}, \sigma\mathcal{L}$ matrices into real matrices so that the state space matrices will be real.

$$Define: \quad I = eye(noports)$$

$$g = \frac{1}{\sqrt{2}} \begin{bmatrix} I & -i*I \\ I & i*I \end{bmatrix}$$

$$G = kron(eye(\frac{N}{2}), g);$$

$$\mathcal{L}_r = G'\mathcal{L}G;$$
$$\sigma\mathcal{L}_r = G'\sigma\mathcal{L}G;$$
$$V_r = G'V;$$
$$W_r = WG;$$

Step 6b: *Identify the order of system*
The Loewner matrix pencil singular values can be used to identify the order of the system. The steps below plot the singular values of the Loewner matrix

$$Define: \quad k1 = \text{any value between } 1 \text{ to } N;$$
$$x = imag\left(\lambda_1\left(k1,1\right)\right);$$
$$[Y, \Sigma, X] = svd\left(x\mathcal{L}_r - s\mathcal{L}_r\right);$$
$$SV = diag\left(\Sigma\right)/\Sigma\left(1,1\right);$$
$$semi\log y\left(SV\right);$$

The order of the system can be selected approximately from the plot where the largest drop in singular values occurs and is denoted as K.

Step 6c: *Formulation of state space model*
From the singular value decomposition the state

7

space model can be formulated as follows

$$Y_K = Y(:,1:K);$$
$$X_K = X(:,1:K);$$
$$E = -Y_K'\mathcal{L}_r X_K;$$
$$A = -Y_K'\sigma\mathcal{L}_r X_K;$$
$$B = Y_K'V_r;$$
$$C = W_r X_K;$$

The realization obtained above sometimes will have unstable poles and the order may not be the true order of the system because of the embedded D matrix in the realization [12]. Stable reduced order model is obtained by using the procedure in [16] which essentially separates the unstable part and fits a first order polynomial to the unstable response as shown below

Step 6d: *Obtains Stable Reduced Order Model*

$$sys = dss(A,B,C,0,E);$$
$$sys = ss(sys,'explicit');$$
$$[sys1\ sys2] = stabsep(sys);$$
$$[A_R\ B_R\ C_R\ D_{R1}] = ssdata(sys1);$$
$$E_R = eye(size(A_R,1),size(A_R,1));$$

Step 6e: *D and Y^∞ extraction using polyfit*

for k = 1 : length(S)
    $s = S(k);$
    $H_U(:,:,k) = H(:,:,k) - C_R(sE_R - A_R)^{-1}B_R;$
end

for k = 1 : p
  for i = 1 : p
      $Pfit = polyfit(S^T, squeze(H_U(k,i,:)),1);$
      $Y^\infty(k,i) = Pfit(1);$
      $D(k,i) = Pfit(2);$
  end
end

Acknowledgment

The author would like to thank Dr. S. Lefteriu for giving valuable information which gave better understanding of the original VFTI method. And also thank Dr.Taku Noda for sharing the test system 2 data.

References

[1] U. Annakkage, N. Nair, Y. Liang, A. Gole, V. Dinavahi, B. Gustavsen, T. Noda, H. Ghasemi, A. Monti, M. Matar, R. Iravani, J. Martinez, Dynamic System Equivalents: A Survey of Available Techniques, IEEE Trans. Power Delivery 27 (1) (2012) 411–420.

[2] A.I. Ibrahim, Frequency dependent network equivalents for electromagnetic transients studies: a bibliographical survey, Electrical Power and Energy Systems 25 (2003) 193–199.

[3] D. Deschrijver, B. Gustavsen, T. Dhaene, Advancements in iterative methods for rational approximation in the frequency domain, IEEE Trans. Power Delivery 22 (3) (2007) 1633–1642.

[4] T. Noda, Identification of a multiphase network equivalent for electromagnetic transient calculations using partitioned frequency response, IEEE Trans. Power Delivery 20 (2) (2005) 1134–1142.

[5] T. Noda, A binary frequency-region partitioning algorithm for the identification of a multiphase network equivalent for emt studies, IEEE Trans. Power Delivery 22 (2) (2007) 1257–1258.

[6] A. Ramirez, Vector fitting-based calculation of frequency-dependent network equivalents by frequency partitioning and model-order reduction, IEEE Trans. Power Delivery 24 (1) (2009) 410–415.

[7] A. Ubolli, B. Gustavsen, Multiport frequency-dependent network equivalencing based on simulated time-domain responses, IEEE Trans. Power Delivery 2 (27) (2012) 648–656.

[8] B. Gustavsen, A. Semlyen, Rational approximation of frequency domain responses by vector flltlng, IEEE Trans. Power Delivery 14 (3) (1999) 1052–1061.

[9] A. Ubolli, B. Gustavsen, Comparison of Methods for Rational Approximation of Simulated Time-Domain Responses: ARMA, ZD-VF, and TD-VF, IEEE Trans. Power Delivery 26 (1) (2011) 279–288.

[10] I. Rahimi Pordanjani, W. Xu, Improvement of vector fitting by using a new method for selection of starting poles, Electric Power Systems Research 107 (2014) 206–212.

[11] K. Sheshyekani, B. Tabei, Multiport Frequency-Dependent Network Equivalent Using a Modified Matrix Pencil Method, IEEE Transactions on Power Delivery 29 (5) (2014) 2340–2348.

[12] A. Mayo, A. Antoulas, A framework for the solution of the generalized realization problem, Linear Algebra and its Applications 425 (2007) 634–662.

[13] S. Lefteriu, A. C. Antoulas, A New Approach to Modeling Multiport Systems from Frequency-Domain Data, IEEE Trans. Computer-Aided Design of Integrated Circuits and Systems 29 (1) (2010) 14–27.

[14] S. Lefteriu, Modeling Systems from Measurements of their Frequency Response, Ph.D. thesis, Rice University (2011).

[15] M. Kabir, R. Khazaka, Macromodeling of Distributed Networks From Frequency-Domain Data Using the Loewner Matrix Approach, IEEE Trans. on Microwave Theory and Techniques 60 (12) (2012) 3927–3938.

[16] G. Gurrala, Loewner matrix approach for modelling FDNEs of power systems, Electric Power Systems Research 125 (2015) 116–123.

[17] Y. Wang, C.-U. Lei, G. K. H. Pang, N. Wong, MFTI: Matrix-Format Tangential Interpolation for Modeling Multi-Port Systems, in: Proc. IEEE/ACM Design Automation Conf., Anaheim, CA,, CA, 2010, pp. 683–686.

[18] Matrix fitting toolbox1, http://www.sintef.no/vectfit.

[19] B. Gustavsen, A. Semlyen, Rational approximation of frequency domain responses by vector fitting, IEEE Trans. Power Delivery 14 (3) (1999) 1052–1061.

[20] B. Gustavsen, Improving the pole relocating properties of vector fitting, IEEE Trans. Power Delivery 21 (3) (2006) 1587–1592.

[21] B. Gustavsen, A. Semlyen, Enforcing passivity for admittance matrices approximated by rational functions, IEEE Trans. Power Sy 16 (1) (2001) 97–104.

[22] B. Gustavsen, H. M. J. D. Silva, Inclusion of Rational Models in an Electromagnetic Transients Program: Y-Parameters, Z-Parameters, S-Parameters, Transfer Functions, IEEE Trans. Power Delivery 28 (2) (2013) 1164–1174.

[23] Y. Wang, Z. Zhang, C.-K. Koh, G. Shi, G. K. H. Pang, N. Wong, Passivity enforcement for descriptor systems via matrix pencil perturbation, IEEE Trans. on Computer-aided Design of Integrated Circuits and Systems 31 (4) (2012) 532–545.